

# Acceleration Test Method for a High Performance Two-Stroke Racing Engine

**Robert J Kee and Gordon P Blair**

Department of Mechanical and Manufacturing Engineering  
The Queen's University of Belfast

## ABSTRACT

This paper describes an inertial dynamometer system which has been applied to the testing of small two-stroke kart racing engines. The dynamometer incorporates a flywheel of appropriate moment of inertia to simulate the mass of a kart and driver. The test procedure involves measurement of the flywheel speed during an acceleration phase resulting from opening the throttle. Calculation of the instantaneous flywheel acceleration corresponding to each engine speed directly gives a measure of the torque and power characteristics. Performance results, including exhaust pressure traces, are presented from a series of tests conducted on a 100 cm<sup>3</sup> kart engine. The results are compared with corresponding steady state measurements recorded on an eddy current dynamometer. In addition, the measured results are compared with predictions from a computer simulation.

## INTRODUCTION

The outstanding features of the crankcase compression two-stroke cycle engine are its high specific power, low weight and mechanical simplicity. Thus, this engine type is well suited to racing applications in vehicles such as motorcycles, karts, snowmobiles and powerboats.

Development and tuning of two-stroke racing engines typically involves a combination of conventional steady state dynamometer testing in the laboratory and timed trials on a racing circuit. However, under typical racing conditions, the engine seldom operates in a steady state condition and engine acceleration rates of up to 7000 rpm/sec are encountered. Since the performance of two-stroke racing engines may be significantly influenced by the acceleration rate of the engine, the value of steady state dynamometer testing is often limited. Hence, greater emphasis is often placed on the timed trials conducted under dynamic racing conditions.

A number of well known difficulties are also encountered during the steady state dynamometer testing of high performance two-stroke engines. The first difficulty is piston seizures due to excessive thermal loading on the piston. Most high performance two-stroke engines operate close to the design limit under racing conditions, where the time-averaged power output from the engine is significantly less than the maximum available from the engine. Consequently, during full load testing, the limits of the engine may be exceeded during the 20 to 30 seconds of running required to record a stable measurement. In order to reduce the likelihood of damage to the engine, the fuel/air mixture is often richened and the ignition timing is retarded. These precautions reduce the thermal loading, but give an unrepresentative measurement of engine performance.

A second difficulty arises due to the dependence of power output on the temperature of the engine and its exhaust system. In the two-stroke engine, the charging of the cylinder, combustion of the mixture and the discharging of exhaust gas are accomplished within one revolution. Consequently, the charging and discharging events overlap and hence the gas flow during these phases is highly dependent on the pressure wave action in the inlet and exhaust tracts. Since the velocities of the waves are in turn dependent on the gas temperatures, it follows that the output of each engine cycle is highly dependent on the temperature characteristics of the gas resident in the exhaust and inlet tracts. In addition, the density of the charge transferred from the crankcase into the cylinder is dependent on the temperature of the inlet tract and the crankcase surfaces. Consequently, this temperature effect, particularly in air-cooled engines, contributes to poor repeatability during steady state testing. Furthermore, during a transient acceleration phase, the instantaneous temperatures corresponding to each engine speed differ from those recorded under steady state conditions. Thus the power developed under steady state

conditions may differ from that produced on the race track. Figure 1 illustrates the influence of cylinder temperature on engine performance.

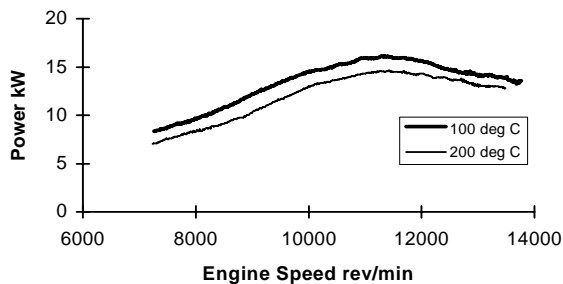


**Fig. 1 Influence of Cylinder Temperature**

A further difficulty arises when the engine is fitted with a mechanical exhaust timing control device, as the response of the mechanism to a change in engine speed will incorporate a finite lag time (1). In order to maximise performance during acceleration, advanced management systems incorporate facilities in which the ignition timing, fuelling and exhaust timing strategies are dependent on the acceleration rate of the engine. For such engines, it is immediately apparent that steady state testing will not provide representative performance characteristics (2).

Finally, steady state testing usually involves measurement of performance at discrete speed intervals of 500 or 1000 rev/min. Occasionally, a significant decrease or 'hole' in the torque characteristic can fall between two measurement speeds.

From the foregoing it is clear that, in addition to the practical difficulties, the optimization of performance under steady state conditions is unlikely to give the optimum characteristics for the dynamic racing situation. Laboratory optimization of high performance two-stroke racing engines ideally requires the use of a technique which reproduces the dynamic conditions of the racing circuit. This paper describes the development and application of a simple and effective dynamic test method which employs the use of an inertial dynamometer.

## KART ENGINE

In the European 100 cm<sup>3</sup> kart racing classes, the crankshaft of the engine is directly coupled to the rear axle by a chain. Consequently the drive ratio is fixed. The rules do not exclude the use of centrifugal clutches, but in practice they are only used by some junior classes. The typical racing circuit is 500 to 1000 meters in length, and usually incorporates one major straight. Since only one drive ratio is available, the engine is required to operate over a wide range of speeds. Typically, the current engines reach speeds above 18000 rev/min at the end of the straight and approximately 6000 rev/min at the slowest corner (3).

The results presented in this paper relate to a reed valve induction engine which is manufactured by the lame

company and marketed under the Sirio brand. The specification of this engine is given in Table 1 and the engine is illustrated in Fig. 2.

**Table 1 Engine Specification**

Engine	Sirio
Bore	50.0 mm
Stroke	50.0 mm
Swept Volume	100 cm <sup>3</sup>
Induction	Reed Valve
Cooling	Air
Exhaust Port Opens	92.5° atdc
Transfer Ports Open	116.5° atdc
Trapped Compression Ratio	10:1
Carburettor Venturi Diameter	19.8 mm
Carburettor Type	Butterfly

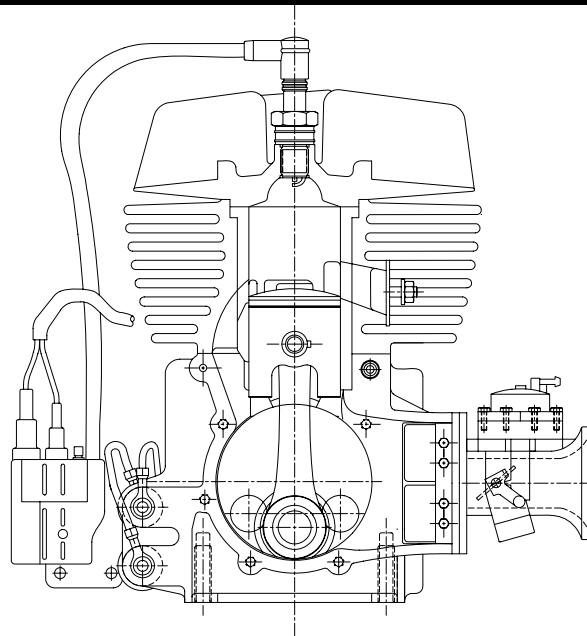


**Fig. 2 100 cm<sup>3</sup> Kart Engine**

## INERTIAL DYNAMOMETER

The inertial dynamometer is an alternative testing system which measures power under acceleration conditions. This method has many attractions, but the transient nature of the test procedure requires the use of a computer and a data acquisition system. The current availability of low cost computer hardware has eliminated this potential drawback.

At The Queen's University of Belfast, an inertial dynamometer has been designed by students as the project element of their engineering degree course. The dynamometer incorporates a flywheel of appropriate moment of inertia to simulate the mass of the kart and driver. The test procedure involves measurement of the flywheel speed during an acceleration phase resulting from opening the engine throttle. Calculation of the

instantaneous flywheel acceleration corresponding to each engine speed directly gives a measure of the torque characteristic. A computer data acquisition system is used to record the flywheel speed and to calculate the performance characteristics.

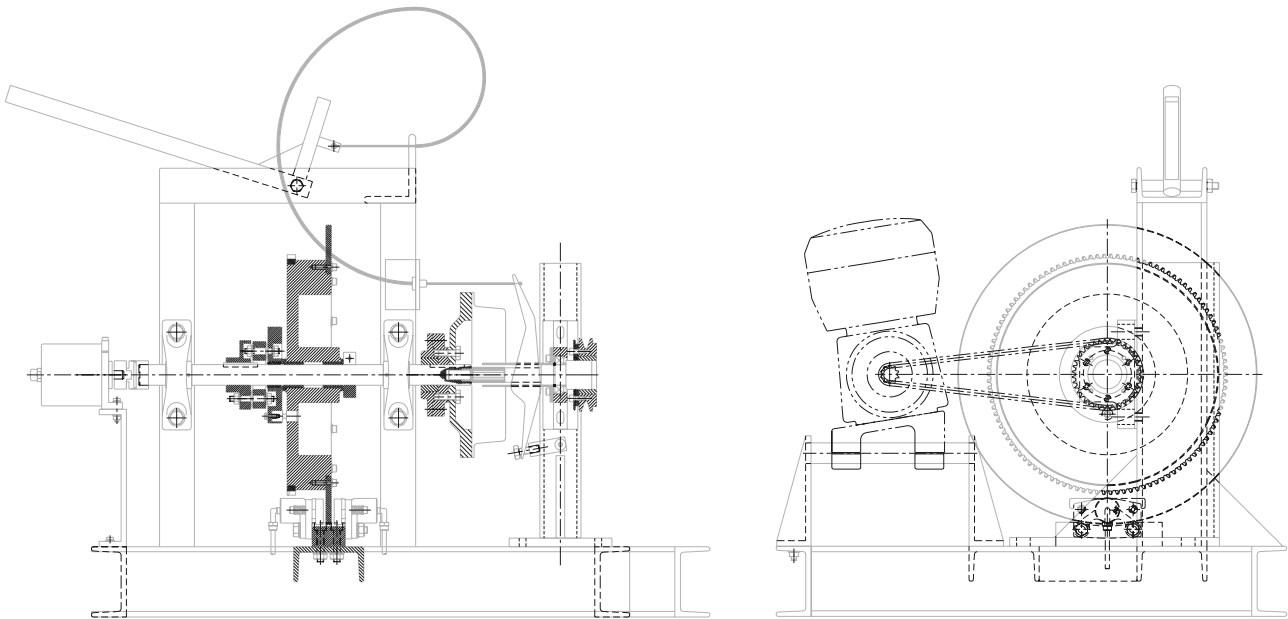
**DYNAMOMETER DESIGN** - The dynamometer incorporates a flywheel which is directly coupled to the engine by a chain as shown in Fig. 3. The chain drives the flywheel via a flexible rubber coupling and a shear pin. The function of the flexible coupling is to introduce compliance into the drive system and thereby reduce the loading on the engine crankshaft due to torque and speed fluctuations. The shear pin is included to reduce damage to the engine in the event of an engine seizure. When the pin breaks, the flywheel will continue to rotate on lubricated bushes and thus the stored energy will not be dissipated through bending and breakage of engine components. A disc brake is incorporated in the design to reduce the flywheel and engine speeds after each test. An automotive clutch allows the flywheel to be accelerated prior to engaging the clutch and starting the engine.

An optical shaft encoder is coupled to the dynamometer flywheel to provide a frequency signal which is converted to an analogue voltage by an integrated circuit. This voltage is proportional to flywheel speed and is connected to one input of a custom designed data acquisition system. A second input channel is used to record the temperature of either the crankcase or the spark plug seat.

The test procedure involves the following:

1. Set engine speed limits for data acquisition (usually 7000 and 16000 rev/min).
2. Start engine.
3. Operate at low speed until the engine temperature measured at the plug seat reaches 75 °C.
4. Switch computer data acquisition system to 'acquire' mode.
5. Open throttle fully and record flywheel speed during the ensuing acceleration.
6. When the maximum engine speed is reached, close throttle.
7. Apply the brake to stop the flywheel.

Analysis functions within the computer programme calculate the engine torque, bmep and power. Figure 5 shows a typical speed characteristic.



NOTE : ENGINE HAS BEEN OMITTED FOR CLARITY

**Fig. 3 Inertial Dynamometer**

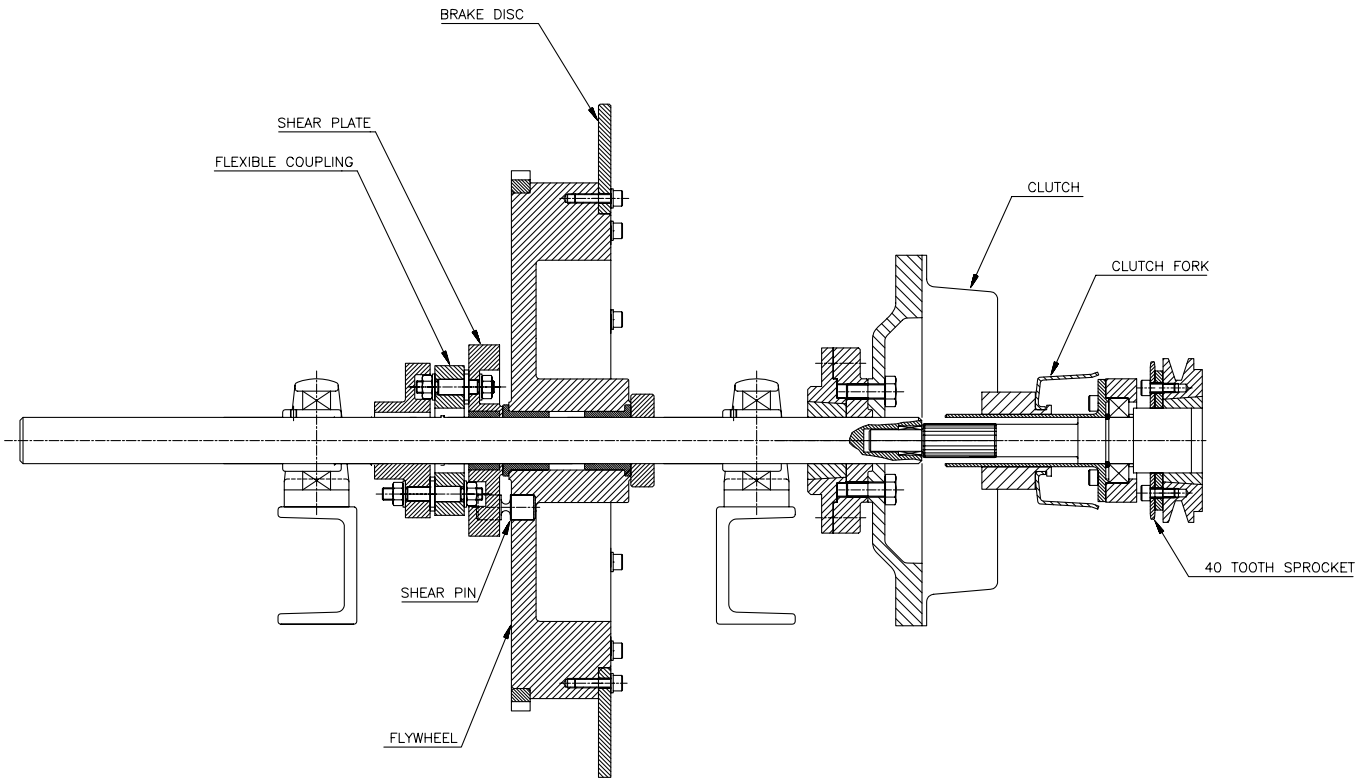


Fig. 4 Shaft Assembly

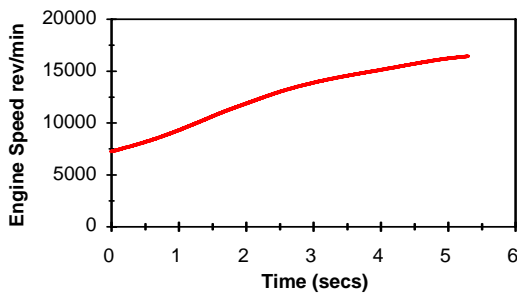


Fig. 5 Typical Engine Speed Characteristic

The torque developed by the engine is calculated by the following equation.

$$T_e = I_f \alpha_e R_f^2 + T_b \quad (1)$$

where

- $\omega_e$  = Engine speed (rad/sec)
- $I_f$  = Flywheel inertia
- $R_f$  = Ratio of flywheel speed to engine speed
- $T_b$  = Torque due to dynamometer bearing friction

The torque due to friction in the dynamometer bearings was calculated from a run-down test. The value was found to be in the range 0.13 to 0.15 Nm. From the torque characteristic, the bmep and power can be easily calculated.

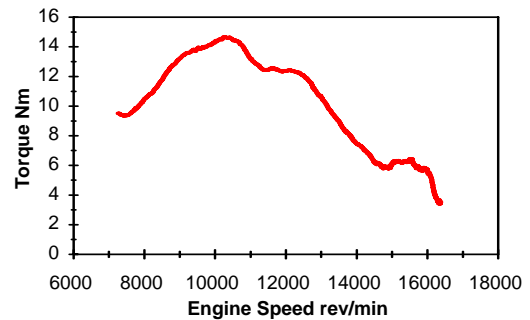
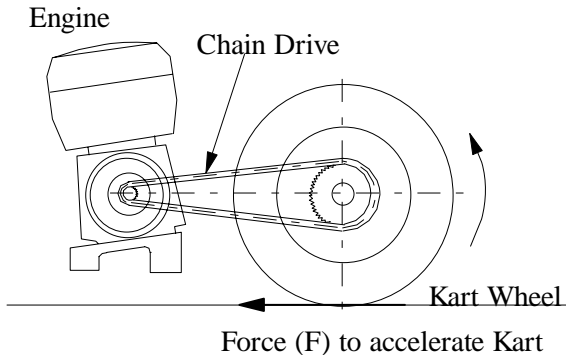


Fig. 6 Typical Torque Characteristic

**FLYWHEEL INERTIA REQUIREMENT** - The dynamometer simulates the loading on a kart racing engine during a typical acceleration period. In a kart, the crankshaft of the engine is directly coupled to the rear axle and thus only one gear ratio is available. This ratio ( $R_k$ ) is defined as the ratio of axle speed to engine speed. During acceleration of the kart due to a torque ( $T_e$ ) applied by the engine, the rate of acceleration is dependent on the mass of the kart ( $m_k$ ), the gear ratio ( $R_k$ ) and the radius of the rear wheels ( $r_w$ ). Neglecting wind resistance and the inertia of the rotating components, the force to accelerate the kart is given by:

$$F = m_k \alpha_e R_k r_w \quad (2)$$



**Fig. 6 Kart Drive System**

The torque applied by the engine is given by:

$$T_e = m_k \omega_e R_k^2 r_w^2 \quad (3)$$

Acceleration of the dynamometer flywheel due to an engine torque ( $T_e$ ) is dependent on the flywheel inertia ( $I_f$ ) and the ratio of flywheel speed to engine speed ( $R_f$ ). Thus,

$$T_f = I_f \omega_f$$

$$\therefore T_e = I_f \omega_e R_f^2 \quad (4)$$

$T_f$  is the torque applied to the flywheel, and  $\omega_f$  is the flywheel speed. For equivalent loading,

$$I_f \omega_e R_f^2 = m_k \omega_e R_k^2 r_w^2$$

$$\therefore I_f = m_k r_w^2 \frac{R_k^2}{R_f^2} \quad (5)$$

The analysis given above has shown that the Moment of Inertia ( $I_f$ ) of the dynamometer flywheel is dependent on the mass of the kart ( $m_k$ ), the radius of the rear wheels ( $r_w$ ), and the gear ratios  $R_k$  and  $R_f$ . The variables  $m_k$  and  $r_w$  are determined by the kart specification and are therefore independent variables.  $R_k$  is dependent on the settings for each circuit - an intermediate value 0.125 was chosen. The design variables are  $I_f$  and  $R_f$ .

As illustrated in Fig. 7, it can be seen that an infinite range of values for  $I_f$  and  $R_f$  will satisfy Eq. 5. Consideration of stresses in the flywheel and clutch assemblies aided in the selection of appropriate values for  $I_f$  and  $R_f$  - 0.81 kgm<sup>2</sup> and 0.25 respectively.

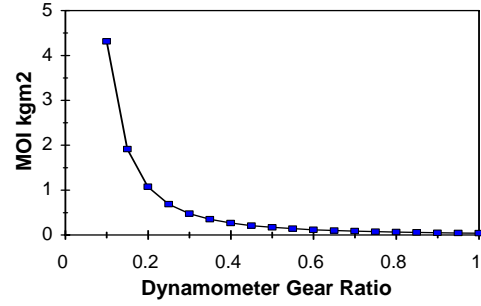


**Fig. 7 Relationship between  $I_f$  and  $R_f$ .**

## ENGINE TESTING

The inertial dynamometer has been used to evaluate the performance of the 100 cm<sup>3</sup> kart engine. Two different exhaust systems were used to illustrate the influence of this component on the performance characteristics. The exhausts are illustrated in Fig. 8 and had identical overall dimensions. The first was a 'stock' exhaust and incorporated a perforated internal convergent cone. The perforations in this cone reduce the amplitude of the reflected pressure wave, and are intended to give a broader torque characteristic. The second exhaust had no perforations and has been designated 'solid'.

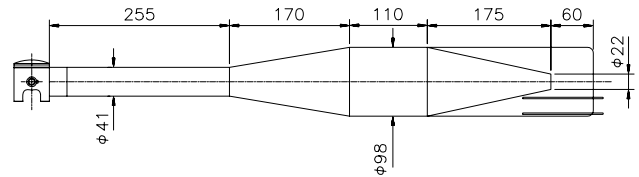


**Fig. 8 Exhaust System**

Comparisons of the power and bmp characteristics are shown in Figs. 9 and 10. These results show that the perforated exhaust gave lower peak values, but a much broader torque characteristic. Examination of the test data shows that the times for acceleration from 6250 to 15500 rev/min were 4.49 and 4.72 seconds for the perforated and solid systems respectively. Thus the broader characteristic of the perforated exhaust gives a time advantage of 0.23 seconds.

Excellent repeatability was noted throughout all the tests conducted on the inertial dynamometer - power and bmp measurements were repeatable to within  $\pm 2\%$ . It is believed that this is due to the standardised test procedure and the small temperature variations which occur during the brief test. Prior to recording results, the engine was warmed up to give a crankcase temperature of 35°C and a temperature of 75°C at the plug seat. During the acceleration test, it was found that the temperatures varied by less than 2°C and 15°C at the crankcase and plug seat respectively.

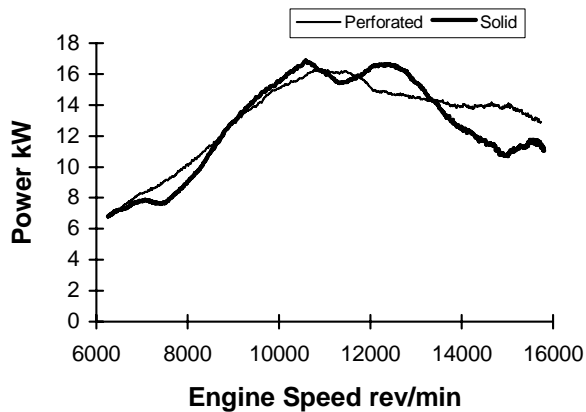


Fig. 9 Comparison of Power Characteristics

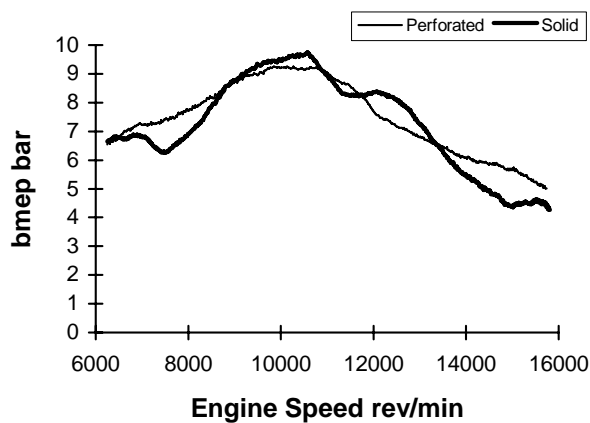


Fig. 10 Comparison of bmep Characteristics

**EXHAUST PRESSURE MEASUREMENTS** - The measurement of exhaust pressure characteristics is an essential element in the optimization of any high performance two-stroke engine. Usually, these measurements are recorded during steady state operation and are fraught with the difficulties discussed earlier in this paper. To avoid these difficulties, an alternative method has been developed which allows pressure traces to be recorded during an acceleration power test on the inertial dynamometer.

Since the system was required to record the cyclic variation of pressure at engine speeds up to 16000 rev/min, relatively high sampling rates were required - at 16000 rev/min, a sampling rate of 96kHz is necessary to give one reading of the pressure and tdc signals for every two degrees of crankshaft rotation. Therefore due to memory limitations, it was not possible to sample continuously at this rate during an acceleration from 6000 to 16000 rev/min. To overcome this limitation, a Computer Boards DAS 330 data acquisition system was configured to sample data at discrete speed intervals. An analogue voltage which was proportional to engine speed was connected to the first input channel of the board and a

customized programme was written to control sampling of the other input channels. When the analogue voltage at the first channel reach a value corresponding to a required speed, data was recorded at the other input channels for a predetermined number of cycles - usually 4. Exhaust pressure data was recorded at 1000 rev/min intervals for speeds from 8000 to 16000 rev/min.

A Kistler type 4045 A5 water cooled piezoresistive transducer was connected via an amplifier and low-pass filter to the second input channel. The filter used was a 4th order low-pass Butterworth type and was tuned to give a cut-off frequency of 2.5 kHz. This filter introduced a group delay of approximately 0.16ms which gave a corresponding phase shift in the pressure measurements. For low speed measurements, this delay corresponds to a small phase shift - 2.9° at 3000 rev/min. However, at 16000 rev/min, the delay corresponds to approximately 15°. In order to reliably evaluate the phase shift, the unfiltered signal was recorded at the third input channel. Finally, a tdc reference signal from a photodiode was connected to the fourth channel. An overall sampling rate of 250kHz was used to give a sampling rate of 62.5kHz for each channel.

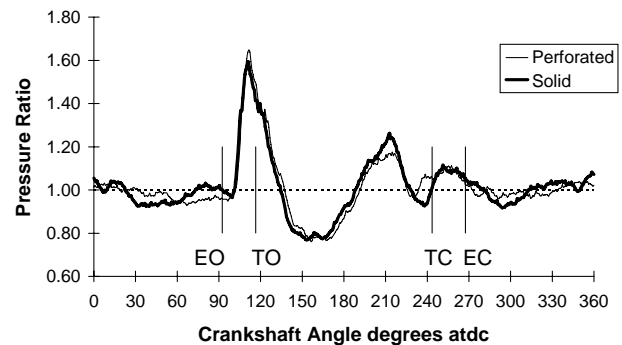


Fig. 11 Comparison of Exhaust Pressures at 8000 rev/min

**RESULTS** - The results presented in Fig. 11 show a comparison of the exhaust pressure traces recorded at 8000 rev/min. The annotations EO, TO, TC and EC denote exhaust open, transfer open, transfer close and exhaust close respectively. It should be noted that the pressure transducer was located 100mm from the exhaust port, thus giving the observed delay between opening of the exhaust port and arrival of the blowdown pulse.

For both exhausts, the reflected plugging pulse is returning to the exhaust port too early to give an effective increase in cylinder pressure at exhaust closure. The early arrival of this pulse also reduces the beneficial influence of the suction pulse which results from reflection of the blowdown pulse from the divergent cone. The resultant effect of the relatively poor trapping pressure and delivery ratio is a torque value well below that produced at the optimum speed for the exhaust system. Comparison of the two characteristics shows that the plugging pulse reflected from the solid cone had a greater amplitude and was

followed by a suction pulse, just prior to exhaust closure. These differences resulted in the 1 bar decrease in bmep noted at 8000 rev/min.

Figures 12 and 13 show exhaust pressure traces recorded at 10000 and 16000 rev/min with the solid cone fitted. These traces illustrate the exhaust pressure wave characteristics at the tuned speed and at a speed well beyond the peak torque point. At 10000 rev/min, a strong suction pulse is followed by a plugging pulse which arrives at the exhaust port just prior to closure. These features maximise both the airflow into the engine and the mass of the charge trapped in the cylinder when the port closes. At 16000 rev/min, it is clear that the plugging pulse arrives after the exhaust port has closed.

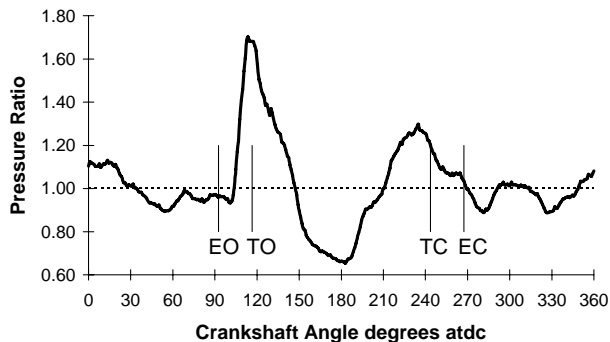


**Fig. 12 Exhaust Pressure at 10000 rev/min**

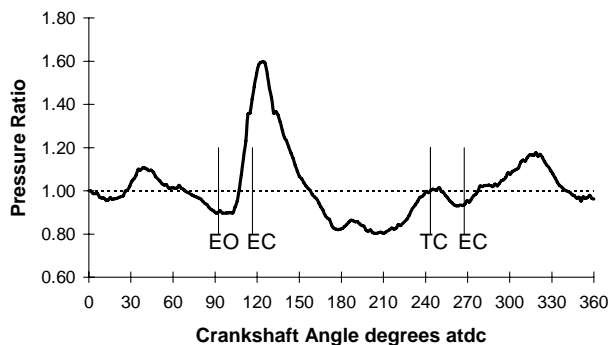


**Fig. 13 Exhaust Pressure at 16000 rev/min**

**STEADY STATE RESULTS** - A comparison of the steady state and acceleration results is presented in Fig. 14. These results show that under steady conditions, the bmep was up to 10% less than that recorded by the inertial dynamometer. It is believed that a number of factors given below have contributed to this result.

1. During steady state testing, the crankcase temperature increased from 35°C to 50°C. The plug seat temperature increased from 75°C to 150°C. These temperature increases occurred despite a cooling down period between each measurement.
2. At the higher speeds, a relatively rich mixture setting was used to prevent seizure of the engine.

3. The control of air/fuel ratio during the acceleration test may differ from that of the steady state condition.
4. The steady state exhaust gas temperatures may be significantly different from those during an acceleration test.

In an effort to ascertain the influence of the final factor, a fast response thermocouple was installed in the mid-section of the exhaust pipe. This thermocouple had a 0.5mm diameter inconel sheath and had a grounded junction to give improved thermal conductivity. The actual response characteristics of the thermocouple have not yet been measured, but in the near future, a single pulse rig will be used to determine the response to a step change in gas temperature.

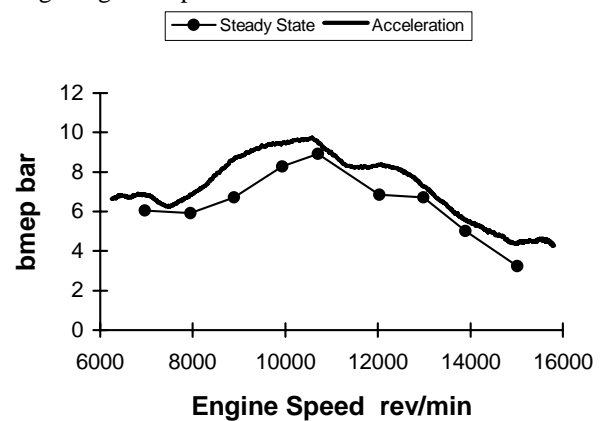


**Fig. 14 Comparison of bmep Characteristics**

The results presented in Fig. 15 show that, for the inertial dynamometer, lower exhaust gas temperatures were recorded between 7000 and 12000 rev/min. For most of this speed range, the lower temperatures will reduce the pressure wave velocity and will give improved exhaust tuning characteristics by delaying the arrival of the plugging pulse. This feature may contribute to the measured bmep difference. Between 13000 and 14000 rev/min, the temperatures are very similar, and the corresponding bmep results also show little variation. Above 14000 rev/min, higher temperatures were recorded on the acceleration test. These higher temperatures will increase the pressure wave velocity and, in this speed range, improved the exhaust tuning effects will result.

The results recorded to date indicate that the two test methods give significant differences in exhaust temperature which in turn produce marked changes in performance. Clearly, further investigation of these exhaust temperature effects is necessary to determine the nature and extent of these phenomena.

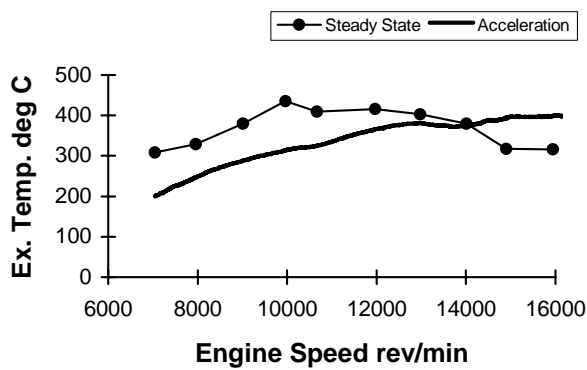


Fig. 15 Comparison of Exhaust Gas Temperatures

## COMPUTER SIMULATION

Today, much of the understanding of physical systems is derived from computer simulations which incorporate mathematical models for the relevant physical processes. Development of these models is often aided by experimental techniques which help identify the important variables, and either provide validation for a theoretical analysis or a basis for an empirical relationship. Hence, a typical simulation model for any complex physical system may comprise interacting theoretical and empirical sub-models which collectively predict the overall response to changes in design or external inputs.

In the case of most reciprocating engines, the basic operating principles are easily understood, and successful engines can be designed without recourse to simulation techniques. However, the fluid dynamics and thermodynamics of the internal processes are extremely complex, and thus in many instances the use of 'cut and try' methods involves excessive experimentation and prototype development. The continual quest for techniques which aid the rapid development of improved engines has provided the stimulus for the study of theoretical simulation techniques. At The Queen's University of Belfast (QUB), the computer modelling of internal combustion engines has been major research topic for over twenty years. The majority of this research has been directed at two-stroke engines, but four-stroke, rotary and gas turbine engines have also been considered.

The two-stroke engine, although mechanically simpler, possesses a greater degree of fluid dynamic complexity than its four-stroke counterpart. During the cylinder blowdown, scavenging and trapping phases, the flow into and out of the cylinder is primarily due to the action of pressure waves, and not cylinder volumetric changes, as in the case of the four-stroke engine. Consequently, the performance characteristics are more markedly influenced by changes in the dimensions of the inlet and exhaust ducts, and the orientation of the ports. For example, on a single-cylinder racing engine, replacement of a tuned exhaust pipe with a straight pipe of

constant cross-section would result in a decrease in peak torque of at least 50%.

In general, the central element in the modelling of reciprocating engines is the simulation of the unsteady gas flow in the inlet and exhaust tracts. In the case of the two-stroke engine, the accurate simulation of unsteady gas flow phenomena is essential. In the exhaust duct, finite amplitude pressure waves result from the release of high pressure exhaust gas; in the inlet, pressure waves result from the volumetric changes in the crankcase volume due to piston motion. Until recently, the 'Method of Characteristics' (5) was primarily used as the basis for simulation of the pressure wave action. However, an alternative method developed by Blair(6) is now employed. This non-isentropic method has been extensively validated on a pressure wave simulator (7) and its claim to accuracy is increasingly supported by correlation with measurements from firing engines.

In the simulation of the two-stroke engine, models are also required to simulate the cylinder scavenging, combustion, heat transfer and port flow processes. In addition, for reed valved two-stroke engines, a model is required to simulate the complex flow characteristics and dynamic action of the reed petals under the action of gas pressure forcing functions. Extensive experimental studies (8,9,10) have led to the development of validated computer models to simulate these elements of the engine's operation.

**KART ENGINE MODEL** - A computer model of the 100cm<sup>3</sup> kart engine was set up to elucidate the wave action phenomena and to aid the future development of improved exhaust systems. The model included detailed geometrical and physical information on all aspects of the engine ducting, cylinder, crankcase, combustion chamber, reed valve, etc. For example, the model of the reed valve included 17 geometrical parameters in addition to the density and Young's modulus of the reed petal material. The exhaust system details used in the computer model were those illustrated in Fig. 8. A solid reverse cone was included as a validated model for the perforated variant is not yet completed.

The computer model predicts the pressure-time histories, mass flow rates and temperatures throughout the engine at discrete crankshaft angle intervals. It is assumed that the engine is operating in a steady state condition and that a constant air/fuel ratio is maintained. During the computation, a graphical display shows the piston position and the variation of the major parameters during each engine cycle. After completion of each cycle, the model generates data for the performance characteristics of bmep, bsfc, delivery ratio, peak cylinder pressure, etc. Stability is attained after 10 to 20 cycles, and the simulation then progresses to the next engine speed.

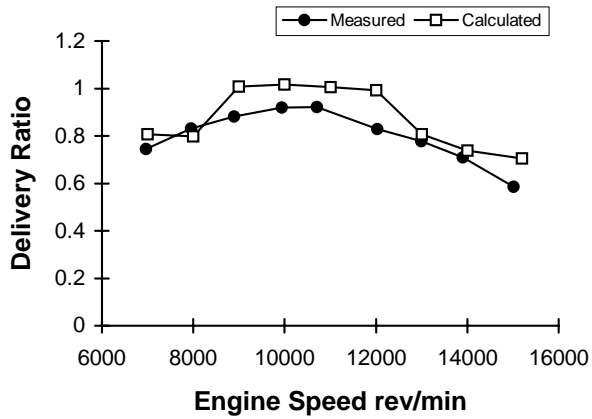


**Fig. 16 Measured and Calculated Delivery Ratio Characteristics**

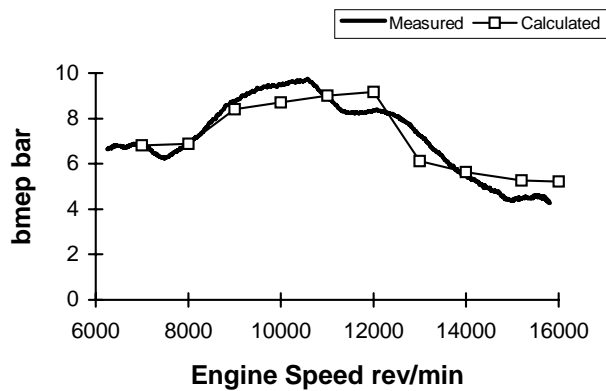


**Fig. 17 Measured and Calculated bmep Characteristics**

**SIMULATION RESULTS** - The measured and calculated delivery ratio characteristics are shown in Fig. 16. Despite the wide range of speeds considered, reasonable correlation is evident. The corresponding bmep characteristics given in Fig. 17 show excellent agreement. A sample plot showing measured and calculated exhaust pressure is presented in Fig. 18. Comparison of the traces shows that all the major features of the measured trace are reproduced by the calculations. The pressures given in Fig. 18 represent the actual dynamic pressure as recorded by a transducer 100mm from the exhaust port. This pressure is the superposition of leftwards and rightwards moving waves which cannot be separated by any instrumentation. However, within the computer model, these waves are calculated independently and graphical output showing each wave can be produced. This feature of the model is often very beneficial in elucidating the exhaust pressure wave action.

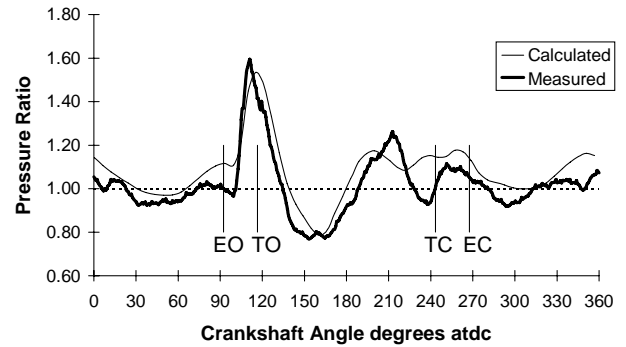


**Fig. 18 Comparison of Measured and Calculated Exhaust Pressures at 8000 rev/min**

## RECOMMENDATIONS AND LIMITATIONS

The inertial dynamometer system described in this paper has proved to be a reliable and useful device. However, in light of the experience gained in designing and operating the dynamometer, a number of possible improvements have become evident. Firstly, the shear pin has proved to be unnecessary, as seizure is extremely unlikely during the brief acceleration period. In the event of a seizure, the clutch can be used to disengage the flywheel. Furthermore, tensile tests on specimens from a kart chain has shown that the chain will break at a relatively low torque level.

The initial design for the dynamometer did not include the automotive clutch, which was added after preliminary tests showed difficulties in starting the engine. Consequently, the addition of the clutch assembly involved a number of design compromises. Clearly, the clutch friction plate could act directly on the main flywheel, thereby eliminating the need for the small secondary flywheel seen in Figs. 3 and 4. The design and manufacture of a more compact dynamometer is currently in progress.

The current limitations of the acceleration test method are the absence of any means to measure air-flow and air/fuel ratio.

## CONCLUSIONS

The design and development of the inertial dynamometer system has proved to be an interesting and challenging project theme for mechanical engineering students. The breadth of the project and the high performance aspects have inspired the students, and excellent commitment and quality of work have resulted. When employed in the testing of a high performance two-stroke engine, the inertial dynamometer has eliminated many of the difficulties encountered during steady state testing, and has provided a test method which more closely represents the conditions of the race track. The addition of a system for recording a series of pressure traces at predetermined engine speeds during a single acceleration

has provided a powerful tool to aid the tuning of engines and the validation of computer simulations.

## ACKNOWLEDGEMENTS

The authors acknowledge The Queen's University for provision of the manufacturing, experimental and computing facilities employed in this study. The contributions of QUB technician Raymond McCullough, students Robin Montgomery, Clive Stewart, Paul McEntee, David Scullion, Peter Turner and Adrian Cunningham, and visiting students Kai, Stephano and Stephane are also gratefully acknowledged. Castrol International Ltd. is acknowledged for supply of the test engine and lubricants.

## REFERENCES

1. **Karl-Heinz Bendix**, 'Optimizing of the nonsteady operational behaviour of high performance two-stroke engines', SAE Paper No. 931509, SETC Conference, Pisa, 1993.
2. **Karl-Heinz Bendix**, 'Optimierung des Instationären Betriebsverhaltens von Hochleistungszweitaktmotoren', 5th International Two-Wheeler Symposium, Technische Universität Graz, Austria, April 1993.
3. **H. Holzleitner**, 'Snowmobile 340ccm Formula 1 - and Kart 100ccm Racing Engines: Two Extremes in Terms of High-Performance Two-Stroke Engine Layouts', SAE Paper No. 911312, 1991.
4. **G.P. Blair**, The Basic Design of Two-Stroke Engines, SAE Publication No. R-104, ISBN 1-56091-008-9, 1990.
5. **R.S. Benson**, The Thermodynamics and Gas Dynamics of Internal Combustion Engines, Volumes 1 and 2, Clarendon Press, Oxford, 1982.
6. **G.P. Blair**, 'An Alternative Method for the Prediction of Unsteady Gas Flow Through the Internal Combustion Engine', SAE International Off-Highway & Powerplant Congress, Milwaukee, Wisconsin, September 1991, SAE Paper No. 911850.
7. **S.J. Kirkpatrick, G.P. Blair, R. Fleck and R.K. McMullan**, 'Experimental Evaluation of 1-D Computer Codes for the Simulation of Unsteady Gas Flow Through Engines - A First Phase', SAE International Off-Highway & Powerplant Congress, Milwaukee, Wisconsin, September 1994, SAE Paper No. 941685.
8. **M.E.G. Sweeney, R.G. Kenny, G.B. Swann and G.P. Blair**, 'Single Cycle Gas Testing Method for Two-Stroke Engine Scavenging', SAE International Congress, Detroit, Michigan, February 1985, SAE Paper No. 850178.
9. **M.G. Reid and R. Douglas**, 'Quasi-Dimensional Modelling of Combustion in a Two-Stroke Cycle Spark Ignition Engine', SAE International Off-Highway & Powerplant Congress, Milwaukee, Wisconsin, September 1994, SAE Paper No. 941680.
10. **R. Fleck, G.P. Blair, R.A.R. Houston**, 'An Improved Model for Predicting Reed Valve Behaviour in Two-Stroke Engines', SAE International Off-Highway & Powerplant Congress, Milwaukee, Wisconsin, September 1987, SAE Paper No. 871654.